

CYTOPLASMIC INCOMPATIBILITY IN POPULATIONS WITH OVERLAPPING GENERATIONS

Michael Turelli

Department of Evolution and Ecology, University of California, Davis, California 95616

E-mail: mturelli@ucdavis.edu

Received April 30, 2009

Accepted August 3, 2009

Many insects and other arthropods harbor maternally inherited bacteria inducing “cytoplasmic incompatibility” (CI), reduced egg hatch when infected males mate with uninfected females. CI-causing infections produce a frequency-dependent reproductive advantage for infected females. However, many such infections impose fitness costs that lead to unstable equilibrium frequencies below which the infections tend to be eliminated. To understand the unstable equilibria produced by reduced lifespan or lengthened development, overlapping-generation analyses are needed. An idealized model of overlapping generations with age-independent parameters produces a simple expression showing how the unstable point depends on the population growth rate, the intensity of CI, and the infection’s effects on development time, longevity, and fecundity. The interpretation of this equilibrium is complicated by age structure. Nevertheless, the unstable equilibrium provides insight into the CI-causing infections found in nature, and it can guide potential manipulations of natural populations, including those that transmit diseases, through the introduction of infections that alter life-table parameters.

KEY WORDS: Age structure, Bartonian waves, population manipulation, unstable equilibria, *Wolbachia*.

Many arthropods, including insects, spiders, and mites, harbor maternally inherited bacteria, assigned to the genera *Wolbachia* and *Cardinium*, that make infected males reproductively incompatible with uninfected females (Hoffmann and Turelli 1997; Werren 1997; Zchori-Fein and Perlman 2004). In diploids, embryos produced from fertilizations of uninfected ova by sperm from infected males typically show significantly lower hatch rates than embryos produced from the three other possible fertilizations. Because the bacteria that cause this cytoplasmic incompatibility (CI) are generally maternally transmitted, CI often produces a reproductive advantage for infected females, leading these infections to spread within and among populations (Turelli and Hoffmann 1991, 1995). However, CI-causing bacteria often produce other phenotypic effects, such as reduced fecundity or longevity (Weeks et al. 2002), that inhibit their spread when they are rare (so that few incompatible matings occur).

Caspari and Watson (1959) first mathematically analyzed the expected frequency dynamics of CI-causing infections. For infections that impose no fitness costs, they found that frequencies should always tend to increase. However, by assuming that the infections might reduce fecundity (an assumption which then had no empirical support), they found that the combination of frequency-dependent reproductive advantage from CI and frequency-independent fecundity costs produced an unstable equilibrium frequency that must be exceeded for the infection frequency to tend to increase. Other fitness costs (or imperfect maternal transmission, Fine 1978; Hoffmann et al. 1990) produce similar “bistable” dynamics, in which both uninfected and (highly) infected populations remain stable to small changes in infection frequency.

Min and Benzer (1997) discovered a *Wolbachia* variant in a laboratory population of *Drosophila melanogaster* that roughly

halves life expectancy (cf. Reynolds et al. 2003). This led Brownstein et al. (2003) to suggest that life-shortening *Wolbachia* might be applied to control vector-borne diseases, such as dengue fever, that are transmitted only by the oldest vector age classes. Although the unstable equilibrium associated with such infections can be approximated numerically (Rasgon et al. 2003; Rasgon and Scott 2004), an analytical treatment can more clearly reveal how the unstable point depends on various demographic factors. Given that relatively few CI-causing infections have been studied thoroughly in nature (Weeks et al. 2002), effects on development time and/or adult longevity may be common. Such effects cannot be understood in terms of the discrete-generation analyses of Caspari and Watson (1959), Fine (1978) or Hoffmann et al. (1990).

I present an analytical treatment of frequency dynamics for CI-causing infections in a random-mating population with overlapping generations, but no age-dependent effects. The analysis illuminates general conditions for bistability and shows how various demographic effects alter the position of the unstable equilibrium. Interpreting this equilibrium is complicated by age structure. Nevertheless, understanding how the unstable point depends on life-table parameters is important, because the position of the unstable point determines whether such infections will tend to spread spatially once they are established in a sufficiently large local population (Barton 1979; Turelli and Hoffmann 1991; Hofbauer 1999). Thus, knowing how the unstable point varies with demographic effects should help us understand natural CI-causing infections and may guide the use of such infections to manipulate natural populations.

Models and Analyses

For algebraic simplicity, I assume perfect maternal transmission, i.e., an infected mother produces only infected eggs. This is a reasonable approximation for mosquitoes in nature carrying single *Wolbachia* infections (Kittayapong et al. 2002; Rasgon and Scott 2003), but not for other taxa, such as *Drosophila simulans* and *D. melanogaster*, whose infected females produce several percent uninfected eggs in nature (Turelli and Hoffmann 1995; Hoffmann et al. 1998). Apart from inducing CI, I assume that these infections affect only fecundity, development time, and/or longevity and that the effects on longevity and development time are sex independent. In fact, *Wolbachia* may affect other aspects of host biology, possibly including mating behavior (Champion de Crespigny and Wedell 2007) and sperm competition (Wade and Chang 1995; Champion de Crespigny and Wedell 2006). All of these complications, including imperfect maternal transmission, can be introduced into the mathematical framework provided, but the resulting equilibrium formulas are much less transparent.

I first introduce and review the standard discrete-generation model with only fecundity effects and CI. This serves as a ref-

erence point for understanding the consequences of overlapping generations. For simplicity, I focus on deterministic dynamics, even though stochastic effects can be important to the initial establishment of infections subject to bistable dynamics (Jansen et al. 2008). Table 1 provides a glossary of notation used throughout the article.

DISCRETE GENERATIONS

In the notation of Hoffmann et al. (1990), the Caspari and Watson (1959) model can be described as follows. Denote infected individuals by I and uninfected by U. Let F denote the average fecundity of an I female relative to a U female. We assume that generally $F \leq 1$, even though *Wolbachia* infections can sometimes increase fecundity (Weeks et al. 2007; Brownlie et al. 2009), and set $s_f = 1 - F$. Let $H < 1$ denote the hatch rate from an incompatible cross, $U\varphi \times I\sigma$, relative to the three other possible crosses, which are assumed to produce equal hatch rates, and set $s_h = 1 - H$. Thus, s_h quantifies the intensity of CI, and s_f quantifies the fecundity cost of the infection. Letting p_t denote the frequency of infected adults in generation t , it is easy to see (e.g., Table 2 of Turelli 1994) that

$$\Delta p = p_{t+1} - p_t = \frac{s_h p_t (1 - p_t) (p_t - \hat{p})}{1 - s_f p_t - s_h p_t (1 - p_t)}, \quad \text{with} \quad (1)$$

$$\hat{p} = s_f / s_h. \quad (2)$$

For initial frequencies below \hat{p} , $p_t \rightarrow 0$ as t increases, whereas for $p_0 > \hat{p}$, $p_t \rightarrow 1$. The unstable point, \hat{p} , is simply the ratio of the fecundity cost to the intensity of CI. For fecundity-enhancing or fecundity-neutral infections (i.e., $F \geq 1$), $s_f \leq 0$; such infections will tend to spread from any initial frequency. In contrast, infections with $s_f > 0$ must somehow get past the unstable point to become established (Jansen et al. 2008). If $s_f \geq s_h$, $\Delta p < 0$ for all $0 < p < 1$, hence only infections with $s_f < s_h$ should be observed in nature, unless the infections provide additional benefits beyond CI (Hoffmann and Turelli 1997; Hedges et al. 2008; Teixeira et al. 2008; Brownlie et al. 2009). As discussed below, a further constraint—roughly that $2s_f < s_h$ —is imposed by the observation that we should find in nature only infections that can spread spatially once they become established locally (Turelli and Hoffmann 1991).

The dynamics in (1) are equivalent to haploid selection with frequency-dependent fitnesses. At equilibrium, infected and uninfected females must produce the same number of progeny, i.e., $F = pH + (1 - p)$, where the left-hand side shows the frequency-independent cost of the infection and the right-hand side shows the frequency-dependent cost of being uninfected. This simple observation, which leads directly to expression (2) for \hat{p} , remains valid with overlapping generations.

Table 1. Glossary of notation.

Symbol	Definition
$b_I (b_U)$	number of female embryos produced by an I (U) female per day
F	fecundity of infected females relative to uninfected females, assuming discrete generations
F_I	expected number of future reproductive I females produced by an I reproductive female each day, $b_I s_I$
F_U	expected number of future reproductive U females produced by a U reproductive female each day in the absence of CI, $b_U s_U$
H	hatch rate from incompatible fertilizations relative to compatible fertilizations, i.e., $1 - (\text{probability of embryo death due to CI})$
I	infected individuals
$I_{A,t}$	number of I reproductive females at time t
$I_{E,t}$	number of newly produced I female embryos at time t
$\lambda_I (\lambda_U)$	asymptotic geometric growth rate of a pure I (U) population
p_t	frequency of I among reproductives at time t , $I_{A,t}/(I_{A,t}+U_{A,t})$
\hat{p}	equilibrium frequency of I among reproductive adults
s_f	$1-F$ with discrete generations, $1-(F_I/F_U)$ with overlapping generations, the fecundity cost (or benefit) of I
s_h	$1-H$, the intensity of CI, i.e., the probability of embryo death due to CI
s_I	probability that a newly produced female I embryo becomes a reproductive adult
s_U	probability that a newly produced female U embryo that does not perish from CI becomes a reproductive adult
s_v	$1 - (\bar{T}_I/\bar{T}_U)$
$\tau_I (\tau_U)$	length of the prereproductive period for U (I) in days beginning with fertilization, reproduction for I (U) begins on day τ_I+1 (τ_U+1)
$\bar{T}_I (\bar{T}_U)$	mean life span of I (U) reproductive adults, $1/(1-v_I)$ [$1/(1-v_U)$]
U	uninfected individuals
$U_{A,t}$	number of U reproductive females at time t
$U_{E,t}$	number of newly produced U female embryos at time t
$v_I (v_U)$	daily survival rate of I_A (U_A) reproductive adults

OVERLAPPING GENERATIONS WITHOUT AGING

Next consider a population with overlapping generations, sampled at discrete times. For such populations, we must track numbers rather than simply frequencies, but I will ignore stochastic effects associated with finite population size, because they simply add unbiased noise to the deterministic dynamics (Haygood and Turelli 2009). My analysis is motivated by the life-shortening popcorn form of *Wolbachia* in *D. melanogaster* (Reynolds et al. 2003), which recently has been transferred to the dengue vector *Aedes aegypti* and shows life-shortening in this novel host comparable to that seen in *D. melanogaster* (McMeniman et al. 2009). Successive sample times will usually be referred to as successive days, but an alternative time unit, "generation time," is convenient for one of the analyses below. A full life-table analysis, as in Rasgon et al. (2003), requires daily survival rates and fecundities for I and U individuals. It could also include age-specific patterns of mating and the effect of infected male age on the level of CI (see, for instance, the *D. simulans* data in Turelli and Hoffmann 1995). However, age-specific survival, fecundity, and mating effects are generally unknown for field populations of *Drosophila* or *Aedes*. Moreover, the field biology of disease vectors is typically summarized by age-independent adult daily survival rates and fecundities, and by estimates of development time from the

onset of embryogenesis to reproductive maturity (Sheppard et al. 1969; Smith et al. 2004).

For simplicity, I assume age-independent reproduction and survival, random mating between all reproductive adults, and equal survival rates and development times for males and females. For most insects, there is a prereproductive adult period; for instance, egg production in *Ae. aegypti* requires a blood meal that typically does not occur until day two or three of adult life. At each time step, we consider only two types of I and U individuals: newly produced female embryos, denoted I_E and U_E , and reproductive adult females, denoted I_A and U_A . Let τ denote the length of the prereproductive period, beginning with fertilization, so that reproduction begins on day $\tau + 1$. For simplicity, I ignore developmental stochasticity (which can be significant in *Ae. aegypti* whose embryos may undergo arrested development associated with desiccation, Christophers 1960) and assume that τ is fixed but may differ between I and U. I assume that (1) all reproductive adults mate at random, irrespective of age or infection status, (2) all I_A (U_A) females produce b_I (b_U) female embryos per day, (3) all I_A (U_A) reproductive adults survive to the next day with probability v_I (v_U), (4) newly produced female I (U) embryos that do not perish from CI become reproductive adults with probability s_I (s_U), (5) all I (U) embryos that survive become

reproductive adults in $\tau_I + 1$ ($\tau_U + 1$) days, and (6) the probability of embryo death due to CI is $1 - H$, irrespective of paternal age.

First consider the dynamics of a population with only infected individuals. Let $I_{E,t}$ denote the number of newly produced female embryos on day t , and let $I_{A,t}$ denote the number of reproductive females. From the definitions, we have

$$I_{E,t} = b_I I_{A,t}. \tag{3}$$

On day $t + 1$, the number of reproductive females is

$$I_{A,t+1} = v_I I_{A,t} + s_I I_{E,t-\tau_I}, \tag{4}$$

where the first term on the right-hand side is the number of adult female survivors from the previous day and the second is the number of newly developed reproductive females. Substituting (3) and defining $F_I = b_I s_I$ (i.e., the expected number of future reproductive females produced by a reproductive female each day), we obtain the recurrence equation

$$I_{A,t+1} = v_I I_{A,t} + F_I I_{A,t-\tau_I}. \tag{5}$$

Using the general theory of age-structured population growth (specifically the Perron–Frobenius theorem, see Caswell 1989, Ch. 4), we know that independent of initial conditions, populations governed by (5) will ultimately grow geometrically, so that

$$I_{A,t} = I_{A,0} \lambda_I^t, \tag{6}$$

where λ_I is the largest positive solution of the characteristic equation

$$\lambda^{\tau_I+1} = v_I \lambda^{\tau_I} + F_I. \tag{7}$$

A monomorphic U population would follow (5) with v_I , F_I and τ_I replaced by v_U , F_U and τ_U ; we denote its asymptotic geometric growth rate by λ_U .

In polymorphic populations, we must account for CI. The number of infected reproductive females still follows (5), because the hatch rate of I offspring does not depend on paternal infection status. In contrast, the relative hatch rate for U embryos is 1 if the father is U, but only H if the father is I. Let p_t denote the frequency of infected mating adults at time t . Under random mating, the number of U adults follows:

$$\begin{aligned} U_{A,t+1} &= v_U U_{A,t} + F_U (H p_{t-\tau_U} + 1 - p_{t-\tau_U}) U_{A,t-\tau_U} \\ &= v_U U_{A,t} + F_U (1 - s_h p_{t-\tau_U}) U_{A,t-\tau_U}, \end{aligned} \tag{8}$$

where $s_h = 1 - H$ as in (1). If we express p_{t+1} as $I_{A,t+1}/(I_{A,t+1} + U_{A,t+1})$, using (5) and (8), we get an intractable expression that depends on values for $I_{A,s}$ and $U_{A,s}$ at times from t back to $s = \min(t - \tau_U, t - \tau_I)$. To produce a simple and interpretable result, we first assume demographic equilibrium, so that the mixed population is growing geometrically, and then recognize that the

relevant geometric growth rate is λ_I . The logic is as follows. If we hold p_t constant, as expected at equilibrium, we can express the asymptotic growth rate of the U population as the largest positive solution of

$$\lambda^{\tau_U+1} = v_U \lambda^{\tau_U} + F_U (1 - s_h p), \tag{9}$$

which we denote $\lambda_U(p)$. Given that the effective fecundity of U females decreases as p increases, it follows that $\lambda_U(p)$ decreases as p increases. For the frequency of I to be at a polymorphic equilibrium, the U and I populations must be growing at the same geometric rate, i.e., there must be a p value for which

$$\lambda_U(p) = \lambda_I. \tag{10}$$

As discussed below, if $\lambda_U(0) = \lambda_U < \lambda_I$ (analogous to $F > 1$ for the discrete-generation model), we expect the infection to spread from any initial frequency; whereas if $\lambda_U(1) > \lambda_I$, the infection should never be able to stably spread (cf. Charlesworth 1984, Sec. 4.3.1).

The equilibrium criterion (10) is relatively uninformative, because the λ are defined implicitly as solutions of the characteristic equations (7) and (9). However, the simple observation made for discrete-generation equilibria remains valid: at equilibrium, the per capita changes of I and U females between successive time steps must be equal, i.e.,

$$\frac{I_{A,t+1}}{I_{A,t}} = \frac{U_{A,t+1}}{U_{A,t}}. \tag{11}$$

This requires

$$v_I + F_I \frac{I_{A,t-\tau_I}}{I_{A,t}} = v_U + F_U (1 - s_h p) \frac{U_{A,t-\tau_U}}{U_{A,t}}. \tag{12}$$

Recognizing that at equilibrium both groups must be growing exponentially at rate λ_I , we have $I_{A,t-\tau_I}/I_{A,t} = \lambda_I^{-\tau_I}$ and $U_{A,t-\tau_U}/U_{A,t} = \lambda_I^{-\tau_U}$. Substituting into (12), we obtain

$$v_I + F_I \lambda_I^{-\tau_I} = v_U + F_U (1 - s_h p) \lambda_I^{-\tau_U}, \tag{13}$$

so that

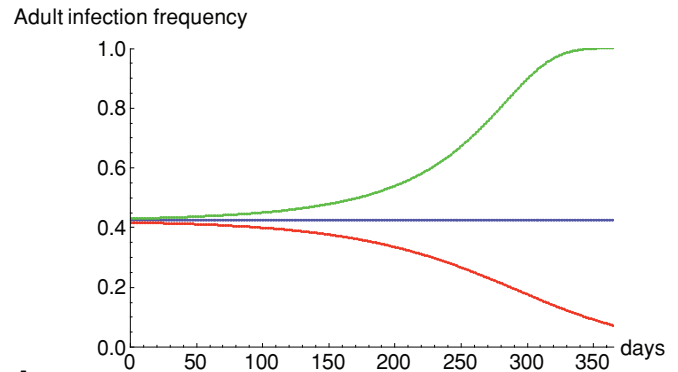
$$\hat{p} = \frac{(v_U - v_I) \lambda_I^{\tau_U} + (F_U - F_I \lambda_I^{\tau_U - \tau_I})}{F_U s_h}. \tag{14}$$

Equation (14) is an overlapping-generation analog of the Caspari and Watson (1959) result $\hat{p} = s_f/s_h$, but there are fundamental differences in the underlying dynamics that complicate its interpretation. The key difference is that recursions (5) and (8) are multidimensional. Hence, their behavior cannot be summarized with simple inequalities analogous to the assertion, valid for (1), that initial frequencies above \hat{p} lead to $p_t \rightarrow 1$ as t increases. To highlight this difference, note that if $0 < \hat{p} < 1$, it is possible to start with no infected reproductive adults, $p_0 = 0$, but have the infection ultimately take over the population, $p_t \rightarrow 1$,

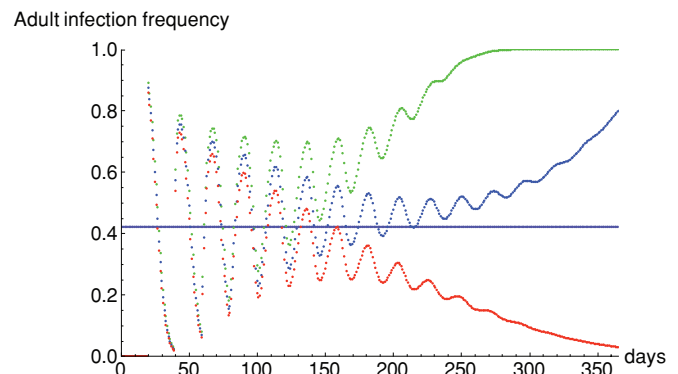
if enough prereproductives are infected. Assuming $\tau_I \geq \tau_U$, we must specify $I_{A,t}$ and $U_{A,t}$ for $\tau_I + 1$ successive time periods to iterate the model described by (5) and (8). We obtained the one-dimensional result (14) only by assuming demographic equilibrium, specifically geometric growth of both $I_{A,t}$ and $U_{A,t}$ at rate λ_I , and assuming that the same (equilibrium) infection frequency held for all time periods. More generally, there is a surface in the $[2(\tau_I + 1) - 1]$ -dimensional space of possible values of the vector $\{I_{A,-\tau_I}, U_{A,-\tau_I}, I_{A,-\tau_I+1}, U_{A,-\tau_I+1}, \dots, I_{A,0}, U_{A,0}\}$ that separates initial values leading to asymptotic fixation of the infection versus asymptotic loss. (Note that the dimension of the space is reduced by 1 because the sum of all of the initial values can be scaled arbitrarily and not affect the final outcome, only the relative frequencies of these $2(\tau_I + 1)$ initial densities matter.) Equation (14) is an informative, but incomplete indicator of asymptotic behavior.

These ideas are illustrated in Figure 1. Both panels are based on iterating (5) and (8) with the same parameter values (corresponding to plausible guesses for *Ae. aegypti* in the field with and without life-shortening *Wolbachia*, based on laboratory estimates from McMeniman et al. 2009 and S. L. O'Neill, pers. comm.): $v_U = 0.850$, $v_I = 0.752$, $F_U = 0.269$, $F_I = 0.255$, $H = 0$, and $\tau_I = \tau_U = 19$. These produce $\lambda_U = 1.023$, $\lambda_I = 1.001$, and $\hat{p} = 0.422$. For Figure 1A, the initial population sizes at successive time points were assumed to increase geometrically at rate λ_I , and the initial frequency of the infection was assumed to be the same over all times. The line is the unstable point, $\hat{p} = 0.422$, given by (14), and Figure 1A shows that for an initial frequency just above \hat{p} , the infection frequency increases, whereas for an initial frequency just below \hat{p} , p_t decreases. This is the precise—and restrictive—sense in which (14) provides the unstable equilibrium frequency.

In contrast, Figure 1B shows the oscillatory adult infection-frequency dynamics resulting when a monomorphic U population, growing geometrically at rate λ_U , is perturbed by introducing a large number of infected reproductive adults on a single day to produce an initial adult infection frequency far above \hat{p} . Because all prereproductives are initially uninfected, the adult infection frequency plummets below \hat{p} as the U prereproductives reach sexual maturity. The ultimate fate of the infection depends on the initial perturbation, and there are several notable features of the dynamics. The dampened fluctuations reflect the approach to a new demographic equilibrium (or “stable age distribution,” SAD). Note that the adult infection frequency, p_t , fluctuates far above and below the unstable point given by (14), and this is seen both for initial conditions that lead to ultimate fixation and ultimate loss of the infection. The starting values were chosen using a heuristic invasion condition that will be described elsewhere. Because of the complexity of the transient dynamics away from SAD, it is difficult to provide a simple analytical formula, analogous to (14),



A



B

Figure 1. Dynamics of adult infection frequencies based on iterating recursions (5) and (8). For both panels, $v_U = 0.850$, $v_I = 0.752$, $F_U = 0.269$, $F_I = 0.255$, $H = 0$, and $\tau_I = \tau_U = 19$, corresponding to $\lambda_U = 1.023$, $\lambda_I = 1.001$, and $\hat{p} = 0.422$ (depicted as a horizontal line in both panels). The two panels differ only in the initial conditions. Panel A assumes that the total population is initially growing geometrically at rate $\lambda_I = 1.001$ and that the initial adult infection frequency is equal for times 1 to 20 ($=\tau_I + 1$). The recursions are iterated from $t = 21$ until $t = 365$. The red curve, depicting loss of the infection, corresponds to an initial infection frequency of 0.415; the green curve, depicting approach to fixation, corresponds to an initial infection frequency of 0.43. Panel B assumes that initially the U population is growing geometrically at rate $\lambda_U = 1.023$. This equilibrium U population is perturbed by introducing only I reproductive adults at $t = 21$. The green trajectory, leading to fairly rapid fixation of I, corresponds to an initial adult infection frequency of 0.89; the blue trajectory, which is just above the critical introduction level that leads to fixation of I, starts with 0.875; and the red, which produces loss of I, starts with 0.86.

for the perturbations of a single age class that will lead to ultimate fixation of the infection.

Conditions for infection fixation, loss, and bistability

Although the dynamics show complex dependence on the high-dimensional initial conditions, some general statements can be made about the long-term fate of infection frequencies. In particular, we can specify when CI-causing infections can always

invade, when they can never invade, and when they can invade only for some initial conditions (bistability). First, note that if $\lambda_U(0) = \lambda_U < \lambda_I$, the infection must ultimately invade once it has been introduced. We will not present a formal proof (see Charlesworth 1984, Sec. 4.3.1 and Appendix 2), but the heuristic argument is as follows. After introduction, the infected population will approach its SAD. If the initial infection frequency is very low, there will be very few incompatible matings. Hence, we will essentially have two competing haploid populations, one growing at rate $\lambda_U(0) = \lambda_U$, the other growing at rate $\lambda_I > \lambda_U$. Thus, the infection frequency will increase, and as it does, $\lambda_U(p)$ will decline, leading to an even greater advantage for I. Conversely if $\lambda_U(1) > \lambda_I$, the infection must vanish; because even when they are very rare, the uninfected individuals will be growing at a geometric rate that exceeds that of the infecteds. Finally, if (10) has a solution between 0 and 1, meaning that $\lambda_U(0) = \lambda_U > \lambda_I$ but $\lambda_U(1) < \lambda_I$, there are some initial conditions from which the infection will spread to fixation and others from which it is lost. Explicit constraints on the parameters that lead to bistability can be obtained from (14) using the inequalities $0 < \hat{p} < 1$.

Special cases

To understand how various demographic factors affect \hat{p} and how (14) relates to the Caspari and Watson (1959) result, $\hat{p} = s_f/s_h$, it is useful to consider some special cases.

Discrete generations

We can collapse recursions (5) and (8) to model nonoverlapping generations by setting $\tau_U = \tau_I = 0$, corresponding to embryos becoming reproductive adults in one time step, and setting $v_U = v_I = 0$, corresponding to no adults surviving for more than one period of reproduction. In this case, the sample-time index t in (5) and (8) is generation number. With these values, (14) becomes

$$\hat{p} = \frac{F_U - F_I}{F_U s_h} = s_f/s_h, \tag{15}$$

Caspari and Watson’s (1959) result. Hence, (5) and (8) generalize (1).

Constant population size: $\lambda_I = 1$

When $\lambda_I = 1$, (14) becomes

$$\hat{p} = \frac{(v_U - v_I) + (F_U - F_I)}{F_U s_h} = \frac{a_v + s_f}{s_h}, \tag{16}$$

where $a_v = (v_U - v_I)/F_U$, and $s_f = 1 - (F_I/F_U)$ is a direct analog of the fecundity-cost parameter in (1). With constant reproductive-adult survival rates, v , the mean life expectancy of reproductive adults is $1/(1 - v)$; when $\lambda_I = 1$, (7) implies that $1 = v_I + F_I$. Thus,

$$\begin{aligned} a_v &= \frac{v_U - v_I}{F_U} = \left(\frac{v_U - v_I}{F_I} \right) \left(\frac{F_I}{F_U} \right) = \left(\frac{v_U - v_I}{1 - v_I} \right) (1 - s_f) \\ &= s_v (1 - s_f), \quad \text{and} \end{aligned} \tag{17a}$$

$$\hat{p} = \frac{s_v + s_f - s_v s_f}{s_h}, \tag{17b}$$

where $s_v = 1 - (\bar{T}_I/\bar{T}_U)$ and \bar{T}_I (\bar{T}_U) is the mean life span of infected (uninfected) reproductive adults. Note that s_v , the fractional reduction of life length for infected individuals, is precisely analogous to s_f , the fractional reduction in daily “effective fecundity.” This special case illustrates the similar consequences of infection costs associated with reduced fecundity versus reduced viability. Conversely, (16) shows how positive *Wolbachia* effects on fecundity (Weeks et al. 2007; Brownlie et al. 2009) can counteract negative viability effects and lower the unstable equilibrium.

Equal fecundities: $F_U = F_I$

Equation (14) becomes

$$\hat{p} = \frac{a_v \lambda_I^{\tau_U} + 1 - \lambda_I^{\tau_U - \tau_I}}{s_h}, \tag{18}$$

where $a_v = (v_U - v_I)/F = s_v(1 - v_I)/F$ and $s_v = 1 - (\bar{T}_I/\bar{T}_U)$ as in (17). If the infection does not affect development time (i.e., $\tau_U = \tau_I = \tau$), this reduces to

$$\hat{p} = a_v \lambda_I^\tau / s_h, \tag{19}$$

illustrating that longevity effects are weighted by the population growth rate and development time.

Equation 19 may suggest that \hat{p} will generally increase with λ_I , but this ignores the joint dependence of λ_I and a_v on the parameters F and v_I . For instance, if we hold v_I , s_v and τ fixed and increase λ_I by raising F , we can use (7) to find the F that produces the desired λ_I . Substituting into (19), we find that $\hat{p} = s_v(1 - v_I)/[s_h(\lambda_I - v_I)]$, which clearly decreases as λ_I increases.

Equal longevitys, $v_U = v_I$

Equation (14) becomes

$$\hat{p} = \frac{F_U - F_I \lambda_I^{\tau_U - \tau_I}}{F_U s_h} = \frac{1 - (1 - s_f) \lambda_I^{\tau_U - \tau_I}}{s_h}, \tag{20}$$

with s_f as in (16). If the infection does not affect development time ($\tau_I = \tau_U$), (20) reduces to the Caspari and Watson (1959) result, $\hat{p} = s_f/s_h$, irrespective of the population growth rate. As discussed below, this simplification may help explain why *Wolbachia* infection-frequency dynamics in California populations of *Drosophila simulans*, which have on the order of 12–15 overlapping generations per year, could be reasonably approximated by a discrete-generation analysis (Turelli and Hoffmann 1995).

OVERLAPPING GENERATIONS WITH AGE-DEPENDENT EFFECTS

With age-dependent infection effects, the model has many parameters and does not seem to produce a simple result analogous to (14), even with random mating. Nevertheless, the principles that led to (14) and the eigenvalue condition for bistability, (10), remain valid after some clarification. With a full age-structured

model, the dynamics (5) and (8) can be recast as iterations of two life-table matrices in which the effective fecundities for the U females depend on the pattern of mating among age classes, age-specific CI effects, and age-specific infection frequencies (see Rasgon et al. 2003). With a fixed vector of age-specific infection frequencies for reproductive adults, denoted \underline{p} , and any pattern of mating, we can calculate how CI alters the effective fecundity of U females who are i days old, denoted $F_{U,i}H(\underline{p})$, by simply averaging the CI values over the appropriate male ages and infection frequencies. Using the life-table parameters, mating pattern, and CI parameters, we can calculate λ_I and $\lambda_U(\underline{p})$ for any fixed \underline{p} .

As in the age-independent case, to get a relatively simple result for the unstable equilibrium, we consider a mixed population growing geometrically at rate λ_I . At this demographic equilibrium, all age classes grow geometrically at rate λ_I . If I adults die faster than U adults, infection frequency will decline with reproductive adult age. However, if we fix the infection frequency for the youngest age class of reproductive adults, denoted p_1 , we can use the I and U viabilities to calculate infection frequencies for all adult age classes. Hence, at this demographic equilibrium, we can view the full distribution of adult infection frequencies, \underline{p} , as a function of a single variable, p_1 . Thus, we can replace (10) by

$$\lambda_U(p_1) = \lambda_I, \quad (21)$$

where the asymptotic growth rates are now obtained from the life-table matrices for U and I.

The condition for bistability, i.e., for the fate of the infection frequency to depend on initial conditions, is that (21) must have a solution between 0 and 1. If $\lambda_U(0) < \lambda_I$, the infection will always invade, whereas if $\lambda_U(1) > \lambda_I$, the infection will never stably invade. By writing explicit recursions for newly produced I and U reproductives in successive days, we can find an equation for \hat{p}_1 that is analogous to (14), but much less obviously informative.

Discussion

As shown above, a simple, analytically tractable model leads to a concise formula for the unstable equilibrium infection frequency, (14), that captures the quantitative effects of life-table changes attributable to CI-causing microbes. The motivation for this analysis is a life-shortening *Wolbachia* whose spread could modify the age structure of host insect populations, specifically disease vectors such as *Ae. aegypti* that transmit disease only at the oldest adult ages (Brownstein et al. 2003; Rasgon et al. 2003). The position and properties of the unstable equilibria are relevant to several questions about both natural *Wolbachia* infections and proposed applications. Central to these considerations is whether an infection will tend to spread spatially once it is established in a sufficiently large patch. A more complete treatment of spatial dynamics will be presented elsewhere. Here I outline some of

the biological issues relating the position of the unstable point to conditions for spatial spread.

SPATIAL SPREAD

First consider the discrete-time model (1). Suppose we begin with a linear array of populations, with all of those to the left of some point infected and all of those to the right uninfected. What happens if the adjacent populations begin exchanging migrants? The infection can either advance to the right, retreat to the left or remain relatively fixed in space. Mathematical predictions depend on the model of migration and the approximations used to describe the bistable dynamics. In analyzing their data on the spatial spread of *Wolbachia* in California populations of *D. simulans*, Turelli and Hoffmann (1991) followed Barton (1979) and used a continuous-time, continuous-space, reaction-diffusion approximation to argue that a “traveling wave” of advancing infection is expected if $\hat{p} < 1/2$. This follows directly from Barton’s (1979) prediction that for underdominant chromosome arrangements, e.g., inversions or translocations in which heterokaryotypes are less fit than either homokaryotype, the more fit homokaryotype (with $\hat{p} < 1/2$) is expected to spread spatially. This result can be generalized from a large body of formal mathematics concerning reaction-diffusion models with bistable dynamics (summarized in Fife (1979, esp. Ch. 4) and Hofbauer (1999)). These analyses assume a continuous-time description for the temporal dynamics and a spatially continuous population with an effectively Gaussian distribution of dispersal distances. If the continuous-time approximation for the frequency dynamics (1) is described by

$$dp/dt = f(p), \quad (22)$$

the temporal-spatial dynamics of the infection frequency can be approximated by a reaction-diffusion model of the form

$$\frac{\partial p(x, t)}{\partial t} = f(p) + \frac{\sigma^2}{2} \frac{\partial^2 p(x, t)}{\partial x^2}, \quad (23)$$

where x denotes the one-dimensional spatial variable and σ is proportional to absolute dispersal distances. This model possesses a traveling wave solution (with invariant shape and constant velocity, cf. Fisher 1937) in which the infection spreads whenever

$$\int_0^1 f(p) dp > 0 \quad (24)$$

(see Fife 1979, Ch. 4 for proof). Turelli and Hoffmann (1991) used a crude approximation that effectively ignored the denominator of (1), so that $f(p) = s_h p(1-p)(p-\hat{p})$. In this case, (24) implies that the infection will tend to spread spatially if and only if the unstable point satisfies $\hat{p} < 1/2$.

More careful approximations indicate that the condition $\hat{p} < 1/2$ is somewhat conservative, in that unstable equilibria slightly above $1/2$ can be compatible with spatial spread. These approximations can be obtained either by using a continuous-time

description for *Wolbachia* dynamics that includes a normalization term analogous to the denominator in (1) or by modeling the interaction of CI and migration in discrete time. This latter approach approximates the temporal-spatial infection frequency dynamics by an integro-difference equation of the form

$$p_{t+1}(x) = \int_{-\infty}^{\infty} k(x - y)h(p_t(y))dy, \quad (25)$$

where $p_t(x)$ denotes the infection frequency at point x in a one-dimensional continuous habitat, $h(p_t(x))$ denotes the local deterministic dynamics for infection frequency (e.g., the recursion $p_{t+1}(x) = h(p_t(x))$ that produces Eq. 1), and $k(x)$ is a symmetric “dispersal kernel” that describes migration distances. Wang et al. (2002) found that (under minimal restrictions on $k(x)$) the infection tends to spread spatially as a traveling wave if and only if

$$\int_0^1 [h(p) - p]dp > 0. \quad (26)$$

This result is directly analogous to (24), because $h(p) - p = \Delta p$. Using model (1), the constraint that (26) imposes on s_f is close to $\hat{p} < 1/2$ when s_h is small, but the discrepancy increases with s_h . Let p^* denote the critical unstable equilibrium value produced by (26). With $s_h = 0.1$, (26) requires $s_f < 0.05026$ (equivalent to $p^* = 0.5026$); whereas when $s_h = 1$, (26) requires $s_f < 0.545$ (equivalent to $p^* = 0.545$).

These alternative approximations are highly idealized descriptions of the population biology of insects such as *D. simulans* and *Ae. aegypti*, whose population dynamics involve, among other things, density regulation at various life stages and seasonally varying parameter values. Hence, we consider the values of the critical point p^* that emerge from alternative approximations as rough guides to the conditions under which CI-causing infections will spread spatially. If \hat{p} , the predicted local, nonspatial, unstable equilibrium is below 0.5, we expect the infections to spread spatially once they are established locally, whereas if the predicted local, nonspatial, unstable equilibrium, \hat{p} , is well above 0.5, e.g., 0.6, we do not expect spatial spread.

As shown numerically by Schofield (2002), the wave speed of an advancing CI-causing infection can depend critically on the form of the dispersal kernel, with faster propagation produced by long-tailed (leptokurtic) dispersal. This reflects a general property of traveling wave models (Wang et al. 2002). In contrast, condition (26) from Wang et al. (2002) shows that the tendency to spread is essentially independent of the shape of the dispersal function.

Spatial dynamics are much more difficult to analyze for age-structured populations (but see Neubert and Caswell 2000). Nevertheless, for age-independent, age-structured population dynamics in space, I conjecture that the position of the unstable point given by (14) can provide a useful guide as to whether

spatial spread is likely to occur. This has been demonstrated for a continuous-time approximation of age-independent effects (S. Schreiber, pers. comm.).

As noted by Barton (1979) (also see Barton and Hewitt 1989), spatial waves associated with bistable dynamics have two important features that distinguish them from those produced by “monostable dynamics” in which frequencies and/or densities tend to increase from all initial values, as in Fisher’s (1937) model of the spread of a uniformly favored allele. The same phenomena are found in ecological models including Allee effects—reduced per capita growth rates at low population density (reviewed in Lewis and Kareiva 1993; Taylor and Hastings 2005). First, unlike “Fisherian waves,” associated with monostable dynamics, which can be initiated by arbitrarily small initial patches carrying the favored allele (or cost-free, CI-causing infection), “Bartonian waves,” associated with bistable dynamics, will propagate only if the infection (or favored underdominant allele) is initially established at a sufficiently high frequency (which must be above the unstable equilibrium) in a sufficiently large patch. Second, unlike Fisherian waves, which merely alter their speed when they encounter environmental inhomogeneities, such as reduced population density or barriers to dispersal, Bartonian waves can be stopped by such inhomogeneities (Barton 1979). Moreover, the magnitude of the inhomogeneity needed to halt spread is proportional to the distance between the actual unstable point, \hat{p} , and the critical value, p^* , produced by (24) or (26). Consequently, as \hat{p} approaches p^* , the expected wave speed slows to zero.

IMPLICATIONS FOR CI-CAUSING INFECTIONS IN NATURE

Several *Wolbachia* infections have been found in nature that reduce fecundity, at least under some conditions; but no *Wolbachia* with significant life-shortening effects analogous to Min and Benzer’s (1997) infection (*wMelPop*) have been collected in the wild. Is this surprising? Note that in the lab, *wMelPop* decreases life length by about one half. If such dramatic life-shortening effects were seen in nature, our results, in particular (16) and (17), lead to unstable points near $\frac{1}{2}$ even with complete CI ($H = 0$). Thus, spatial spread would be at best extremely slow, unless there were favorable CI-independent *Wolbachia* effects that ameliorate the deleterious effects of life-shortening. Hence, it’s not surprising that *wMelPop* was discovered in the laboratory, not nature. Moreover, because CI falls very rapidly with male age in *D. melanogaster* (Hoffmann et al. 1998), such an infection could not take over a population with uninfecteds, no matter how many were introduced. Because the frequency-independent life-shortening is so much greater than the reproductive advantage that accrues from the very low level of CI in this species, such infections can persist only in monomorphic laboratory populations.

WOLBACHIA IN CALIFORNIA *D. SIMULANS*

Our simplified age-structure analysis provides some insight into the fact that a discrete-generation model with three parameters (CI intensity, fecundity effects and imperfect maternal transmission; Hoffmann et al. 1990) reasonably approximates the population dynamics, equilibrium frequencies and evolution of the CI-causing *Wolbachia* infection in California populations of *Drosophila simulans* (Turelli 1994; Turelli and Hoffmann 1995; Weeks et al. 2007; Haygood and Turelli 2009). Laboratory experiments have found no appreciable effects of this infection on either development time or adult longevity (Hoffmann et al. 1990). Because *Wolbachia* effects in these populations seem to be magnified in the laboratory relative to nature (Hoffmann et al. 1990; Turelli and Hoffmann 1995), it is reasonable to conjecture that neither development time nor viability are affected in the wild. Without such effects, our model produces the same equilibrium, (20), with and without overlapping generations. The analogy is not precise, because the intensity of CI in *D. simulans* varies significantly with male age (Hoffmann et al. 1986; Turelli and Hoffmann 1995). Nevertheless, result (20) suggests why age-structure may not be critical to understanding these populations.

POSSIBLE APPLICATIONS

This analysis was motivated by a proposal to use life-shortening *Wolbachia* to modify age structures of the mosquito populations that transmit dengue fever (Brownstein et al. 2003; Rasgon et al. 2003). Large-scale cage trials are currently underway to determine whether the mosquitoes infected with life-shortening *Wolbachia* will satisfy the conditions that will allow these infections to spread. Our analyses indicate the obstacles faced by this strategy. From (16) and (17), we find that if the infections roughly halve life span, as seen under some laboratory conditions (McMeniman et al. 2009), the unstable equilibrium would be near $\frac{1}{2}$. Hence, unless life-shortening is less extreme under field conditions or there are beneficial *Wolbachia* effects that reduce the unstable equilibrium below that predicted from life-shortening alone, the expected spread in nature would be at best very slow. However, if *Wolbachia* without significant life-shortening effects can directly inhibit the growth of the dengue RNA viruses in their vectors (as suggested by results in *D. melanogaster*, Hedges et al. 2008; Teixeira et al. 2008), the introduction threshold for such “protective” *Wolbachia* should be relatively low.

If life-shortening infections are established in nature, the maternally inherited *Wolbachia* should evolve to minimize fitness costs to their hosts (Prout 1994; Turelli 1994; Haygood and Turelli 2009). Rapid evolution of *Wolbachia* towards mutualism has been observed in California populations of *D. simulans*—on the order of a decade or two (Weeks et al. 2007), but this rapid evolution may have required a much longer period in which genetic variation accumulated in the *Wolbachia* population. Comparative

genomic analyses are now underway to describe variation among the *Wolbachia* infecting California *D. simulans*. In contrast to the unknown initial conditions that produced rapid *Wolbachia* evolution in California, field releases of laboratory-transfected *Ae. aegypti* will begin with a single *Wolbachia* type introduced into a few embryos via microinjection (McMeniman et al. 2009). Thus, we might expect some lag before evolutionary amelioration of host-deleterious effects. This evolution would also be delayed if life-shortening effects were restricted to the oldest age classes, which contribute little to future generations (cf. Read et al. 2009). At the opposite extreme, if *Wolbachia* without significant life-shortening effects can directly inhibit growth of dengue viruses in vectors, *Wolbachia* evolution towards mutualism would tend to help rather than hinder disease control.

Given the ubiquity of *Wolbachia* infections and the benign nature of age-structure modification relative to attempts to eradicate vector populations, life-shortening *Wolbachia* provide an attractive potential tool to deal with insect disease-vectors and crop pests whose deleterious effects manifest only late in adult life. Even more promising are introductions of *Wolbachia* that have minimal effects on life-table parameters, but reduce or eliminate the deleterious effects of their hosts.

ACKNOWLEDGMENTS

This research was supported in part by grants from the Foundation for the National Institutes of Health through the Grand Challenges in Global Health Initiative of the Bill and Melinda Gates Foundation and the National Science Foundation (DEB 0815145). I am grateful to N. H. Barton, J. Lipkowitz, S. L. O’Neill, J. Schraiber, S. J. Schreiber, R. L. Unckless, and one extraordinarily conscientious anonymous reviewer for discussions of this research and important comments on previous drafts.

LITERATURE CITED

- Barton, N. H. 1979. The dynamics of hybrid zones. *Heredity* 43:341–359.
- Barton, N. H., and G. M. Hewitt. 1989. Adaptation, speciation and hybrid zones. *Nature* 341:497–503.
- Brownlie, J. C., B. N. Cass, M. Riegler, J. J. Witsenburg, I. Itube-Ormaetxe, E. A. McGraw, and S. L. O’Neill. 2009. Evidence for metabolic provisioning by a common invertebrate endosymbiont, *Wolbachia pipientis*, during periods of nutritional stress. *PLoS Pathogens* 5:e1000368.
- Brownstein, J. S., E. Hett, and S. L. O’Neill. 2003. The potential of virulent *Wolbachia* to modulate disease transmission by insects. *J. Invert. Path.* 84:24–29.
- Caspari, E., and G. S. Watson. 1959. On the evolutionary importance of cytoplasmic sterility in mosquitoes. *Evolution* 13:568–570.
- Caswell, H. 1989. Matrix population models. Sinauer Associates, Sunderland, MA.
- Champion de Crespigny, F. E., and N. Wedell. 2006. *Wolbachia* infection reduces sperm competitive ability in an insect. *Proc. R. Soc. B.* 273:1455–1458.
- . 2007. Mate preferences in *Drosophila* infected with *Wolbachia*. *Behav. Ecol. Sociobiol.* 61:1229–1235.
- Charlesworth, B. 1984. Evolution in age-structured populations, Second Ed. Cambridge Univ. Press, Cambridge, UK.

- Christophers, S. R. 1960. *Aedes aegypti* (L.), the yellow fever mosquito: its life history, bionomics, and structure. Cambridge Univ. Press, Cambridge, UK.
- Fife, P. C. 1979. Mathematical aspects of reacting and diffusing systems. Springer-Verlag, Berlin.
- Fine, P. E. M. 1978. Dynamics of symbiote-dependent cytoplasmic incompatibility in Culicine mosquitoes. *J. Invert. Path.* 31:10–18.
- Fisher, R. A. 1937. The wave of advance of advantageous genes. *Ann. Eugen.* 7:355–369.
- Haygood, R., and M. Turelli. 2009. Evolution of incompatibility-inducing microbes in subdivided host populations. *Evolution* 63:432–447.
- Hedges, L. M., J. C. Brownlie, S. L. O'Neill, and K. N. Johnson. 2008. *Wolbachia* and virus protection in insects. *Science* 322:702.
- Hofbauer, J. 1999. The spatially dominant equilibrium of a game. *Ann. Oper. Res.* 89:233–251.
- Hoffmann, A. A., and M. Turelli. 1997. Cytoplasmic incompatibility in insects. Pp. 42–80 in S. L. O'Neill, A. A. Hoffmann and J. H. Werren, eds. *Influential passengers*. Oxford Univ. Press, Oxford, UK.
- Hoffmann, A. A., M. Turelli, and G. M. Simmons. 1986. Unidirectional incompatibility between populations of *Drosophila simulans*. *Evolution* 40:692–701.
- Hoffmann, A. A., M. Turelli, and L. G. Harshman. 1990. Factors affecting the distribution of cytoplasmic incompatibility in *Drosophila simulans*. *Genetics* 126:933–948.
- Hoffmann, A. A., M. Hercus, and H. Dagher. 1998. Population dynamics of the *Wolbachia* infection causing cytoplasmic incompatibility in *Drosophila melanogaster*. *Genetics* 148:221–231.
- Jansen, V. A. A., M. Turelli, and H. C. J. Godfray. 2008. Stochastic spread of *Wolbachia*. *Proc. R. Soc. Lond. B.* 275:2769–2776.
- Kittayapong, P., K. J. Baisley, R. G. Sharpe, V. Baimai, and S. L. O'Neill. 2002. Maternal transmission efficiency of *Wolbachia* superinfections in *Aedes albopictus* populations in Thailand. *Am. J. Trop. Med. Hyg.* 66:103–107.
- Lewis, M. A., and P. Kareiva. 1993. Allee dynamics and the spread of invading organisms. *Theor. Pop. Biol.* 43:141–158.
- McMeniman, C. J., R. V. Lane, B. N. Cass, A. W. C. Fong, M. Sidhu, Y. Wang, and S. L. O'Neill. 2009. Stable introduction of a life-shortening *Wolbachia* infection into the mosquito *Aedes aegypti*. *Science* 323:141–144.
- Min, K. T., and S. Benzer. 1997. *Wolbachia*, normally a symbiont of *Drosophila*, can be virulent, causing degeneration and early death. *Proc. Natl Acad. Sci. USA* 94:10792–10796.
- Neubert, M. G., and H. Caswell. 2000. Demography and dispersal: calculations and sensitivity analysis of invasion speed for structured populations. *Ecology* 81:1613–1628.
- Prout, T. 1994. Some evolutionary possibilities for a microbe that causes incompatibility in its host. *Evolution* 48:909–911.
- Rasgon, J. L., and T. W. Scott. 2003. *Wolbachia* and cytoplasmic incompatibility in the California *Culex pipiens* mosquito species complex: parameter estimates and infection dynamics in natural populations. *Genetics* 165:2029–2038.
- . 2004. Impact of population age structure on *Wolbachia* transgene driver efficacy: ecologically complex factors and release of genetically modified mosquitoes. *Insect Biochem. Mol. Biol.* 34:707–713.
- Rasgon, J. L., L. M. Styer, and T. W. Scott. 2003. *Wolbachia*-induced mortality as a mechanism to modulate pathogen transmission by vector arthropods. *J. Med. Entomol.* 40:125–132.
- Read, A. F., P. A. Lynch, and M. B. Thomas. 2009. How to make evolution-proof insecticides for malaria control. *PLoS Biol.* 7:e1000058.
- Reynolds, K. T., L. J. Thomson, and A. A. Hoffmann. 2003. The effects of host age, host nuclear background and temperature on phenotypic effects of the virulent *Wolbachia* strain popcorn in *Drosophila melanogaster*. *Genetics* 164:1027–1034.
- Schofield, P. 2002. Spatially explicit models of Turelli–Hoffmann *Wolbachia* invasive wave fronts. *J. Theor. Biol.* 215:121–131.
- Sheppard, P. M., W. W. MacDonald, R. J. Tonn, and B. Grab. 1969. The dynamics of an adult population of *Aedes aegypti* in relation to dengue hemorrhagic fever in Bangkok. *J. Anim. Ecol.* 38:661–702.
- Smith, D. L., J. Dushoff, and F. E. McKenzie. 2004. The risk of a mosquito-borne infection in a heterogeneous environment. *PLoS Biol.* 2:1957–1964.
- Taylor, C. M., and A. Hastings. 2005. Allee effects in biological invasions. *Ecol. Lett.* 8:895–908.
- Teixeira, L., A. Ferreira, and M. Ashburner. 2008. The bacterial symbiont *Wolbachia* induces resistance to RNA viral infections in *Drosophila melanogaster*. *PLoS Biol.* 6:2753–2763.
- Turelli, M. 1994. Evolution of incompatibility-inducing microbes and their hosts. *Evolution* 48:1500–1513.
- Turelli, M., and A. A. Hoffmann. 1991. Rapid spread of an inherited incompatibility factor in California *Drosophila*. *Nature* 353:440–442.
- . 1995. Cytoplasmic incompatibility in *Drosophila simulans*: dynamics and parameter estimates from natural populations. *Genetics* 140:1319–1338.
- Wade, M. J., and N. W. Chang. 1995. Increased male fertility in *Tribolium confusum* beetles after infection with the intracellular parasite *Wolbachia*. *Nature* 373:72–74.
- Wang, M.-H., M. Kot, and M. G. Neubert. 2002. Integrodifference equations, Allee effects, and invasions. *J. Math. Biol.* 44:150–168.
- Weeks, A. R., K. T. Reynolds, and A. A. Hoffmann. 2002. *Wolbachia* dynamics and host effects: what has (and has not) been demonstrated? *Trends Ecol. Evol.* 17:257–262.
- Weeks, A. R., M. Turelli, W. R. Harcombe, K. T. Reynolds, and A. A. Hoffmann. 2007. From parasite to mutualist: rapid evolution of *Wolbachia* in natural populations of *Drosophila*. *PLoS Biol.* 5:997–1005.
- Werren, J. H. 1997. Biology of *Wolbachia*. *Ann. Rev. Entomol.* 42:587–609.
- Zchori-Fein, E., and S. J. Perlman. 2004. Distribution of the bacterial symbiont *Cardinium* in arthropods. *Mol. Ecol.* 13:2009–2016.

Associate Editor: C. Jiggins